Direct Numerical Simulation of Turbulence Structure and CO_2 Transfer Mechanism at the Air-Sea Interface

Contact Person	Associate Professor, Satoru Komori Dept. of Chemical Engineering, Kyushu University
(Research Organization)	PhD Student, Ryuichi Nagaosa Dept. of Chemical Engineering, Kyushu University
	MC Student, Ryoichi Kurose Dept. of Chemical Engineering, Kyushu University
	Section Head, Shunji Takeshita National Institute for Environmental Studies, Environmental Agency of Japan

Keywords: global warming, CO_2 budgets, CO_2 transfer, air-water interface, direct numerical simulation, turbulence structure

1.Introduction

Mass transfer mechanism across wind-driven wavy air-water interfaces is of great practical interest in estimating CO_2 exchange rate across the air-sea interface. Transfer velocity of CO_2 across wind-driven wavy air-water interfaces have been measured by a number of investigators through laboratory and field experiments. However, the data of gas transfer velocity have been very much scattered among individual studies and they have roughly showed the linear proportionality between transfer velocity and wind friction velocity or wind speed on the logarithmic graph. Furthermore, most previous studies have tried only to correlate the transfer velocity with wind shear or wind speed, and they have not physically explained what mechanism controls CO_2 transfer across wavy interfaces. This has been attributed to the fact that it is very difficult to experimentally investigate the turbulence structure near the moving air-water interface. However, to clarify the CO_2 transfer mechanism, it is quite necessary to investigate the turbulence structure near the wavy air-water interface by means of the turbulent velocity measurements [1-4].

The purpose of this study is to numerically investigate both the turbulent structure near a wavy air-water interface where turbulence is generated only by the wind shear and the effect of the wind shear on the CO_2 transfer across the wavy sheared interface. Turbulent velocity field was computed by means of a three dimensional direct numerical simulation (DNS) based on the finite difference method. Here some results obtained from the DNS are reported.

2.Direct Numerical Simulation (DNS)

The coordinate system which can describe the free surface is shown in Fig.1. Subscripts 1,2 and 3 denote the streamwise, spanwise, and vertical direction, respectively. The equations governing the flow in an incompressible Newtonian fluid are

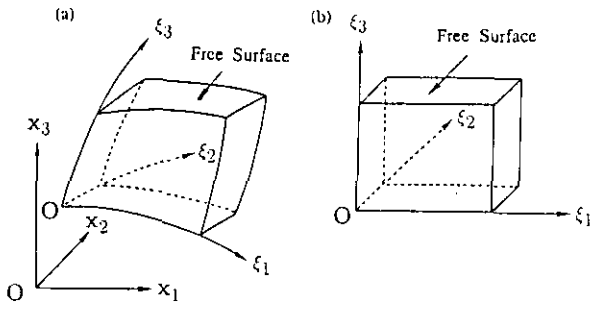

Figure 1: The coordinate system used in this study: (a)physical region; (b)computational region.

$$\frac{\partial v_i}{\partial x_i} = 0, \qquad \text{(Continuity equation)} \quad (1)$$

$$\frac{\partial v_i}{\partial t} + v_j \frac{\partial v_i}{\partial x_j} = -\frac{1}{\rho}\frac{\partial p}{\partial x_i} + \nu \frac{\partial^2 v_i}{\partial x_j \partial x_j} + g\delta_{i3}$$

(Navier-Stokes equation) (2)

where v_i is the ith component of the velocity vector, p is the pressure, ν is the kinematic viscosity, g is the acceleration of gravity, ρ is the density and δ_{ij} denotes the Kroneker's delta. The Einstein summation convention is also used. In both streamwise and spanwise directions, the periodic boundary condition was used for all velocities and pressure. The boundary condition enables us to treat an open-channel flow in the

finite flume as a free surface flow on the infinite plane. On the free surface, two boundary conditions should be satisfied. One is the kinematic boundary condition[Eq.(3)] which describes the Lagrangian behavior of the fluid particle on the free surface, and the other is the dynamical boundary condition [Eqs.(4) and (5)] which is determined from the balance of the stresses acting on the interface in the normal and tangential directions:

$$\frac{\partial F}{\partial t} + v_i \frac{\partial F}{\partial x_i} = 0 \tag{3}$$

$$\left.\begin{aligned} p + \sigma_n + p_s &= p_0 \\ \sigma_n &= \mu e_{ij} n_j n_i \\ p_s &= \gamma \kappa_m \end{aligned}\right\} \tag{4}$$

$$\sigma_t = \mu e_{ij} n_j t_i = 0 \tag{5}$$

where $F, \sigma_n, p_s, p_0, \mu, e_{ij}, n_i, \gamma, \kappa_m, \sigma_t$ and t_i are, respectively, the function displaying the form of the free surface, the normal component of the viscous force vector, the pressure variation by the surface tension, the pressure on the gas side, the viscosity, the deformation rate tensor, the unit vector in the normal direction, the surface tension, the mean curvature on the free surface, the tangential component of viscous force vector, and the unit vector in the tangential direction.

Introducing the characteristic velocity and length, V and L, we obtain a set of the reference values;

$$\begin{aligned} &v^* = \frac{v}{V}, \quad x^* = \frac{x}{L}, \quad p^* = \frac{p}{\rho V^2}, \\ &Re = \frac{VL}{\nu}, \quad Fr = \frac{V^2}{gL} \quad \gamma^* = \frac{\gamma}{\rho L V^2}, \\ &e_{ij}^* = e_{ij}\frac{L}{V}, \quad \kappa_m^* = \kappa_m L, \quad F^* = \frac{F}{L}, \\ &t^* = \frac{t}{L/V}. \end{aligned} \tag{6}$$

Substitution of Eqs.(6) into Eqs.(1)-(5) and the omission of the asterisks leads to

$$\frac{\partial v_i}{\partial x_i} = 0, \tag{7}$$

$$\frac{\partial v_i}{\partial t} + v_j \frac{\partial v_i}{\partial x_j} = -\frac{\partial P}{\partial x_i} + \frac{1}{Re}\frac{\partial^2 v_i}{\partial x_j \partial x_j}, \qquad P = p - \frac{1}{Fr}(x_3 - x_{30}), \tag{8}$$

$$\frac{\partial F}{\partial t} + v_i \frac{\partial F}{\partial x_i} = 0, \tag{9}$$

$$p + \frac{1}{Re} e_{ij} n_j n_i + \gamma \kappa_m = p_0, \tag{10}$$

$$\sigma_t = e_{ij} n_j t_i, \tag{11}$$

where the pressure P is the reference pressure involving the effect of the gravity, and x_{30} denotes the height of the reference position which corresponds to the averaged interface.

The details of the numerical procedure are given in Ref.5.

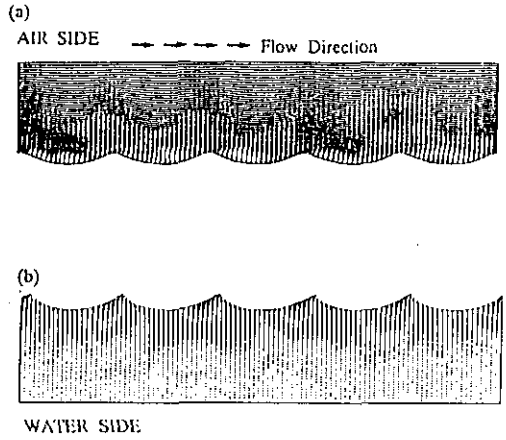

Figure 2: Instantaneous velocity vectors in wind wave turbulence: (a)air side; (b)water side.

3.Results and Discussion

Figure 2 shows the instantaneous velocity vectors in both air and water flows. From the velocity vectors together with the flow visualization in a wind-wave tank[1] we can get a sketch of the organized motions near the wavy sheared air-water interface, as shown in Fig.3. The organized motion in the air flow above the interface intermittently appears in front of the wave crest. The organized motion in the air flow above the highly sheared wavy interface is generated by the wave. The generation mechanism will be different from the bursting phenomena observed near the smooth rigid wall, since the intermittent organized motion is always observed in front of the wave crest as sketchd in Fig.3. As shown in Figs.4 and 5 the instantaneous shear stress and pressure become maximum in front of the wave crest, and the motion is accelerated above the crest in the outward direction. On the water side the surface-renewal motion intermittently and frequently appears, and it renews the free surface like as a rolling eddy. The frequency of the appearance of the surface-renewal eddy in the high shear region is far larger than the typical frequency of the waves and the scale of the

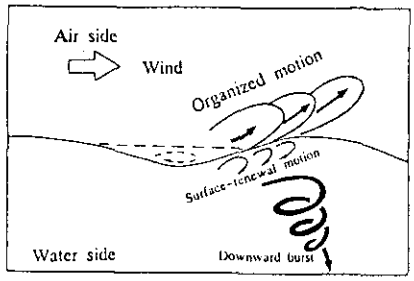

Figure 3: A sketch of turbulence structure near the wavy sheared air-water interface.

surface-renewal eddy is roughly estimarted to be $0.05 \sim 0.50\ \lambda$. Here λ is the wavelength. Also the surface-renewal motion is observed to be generated below the interface at the same place where the organized motion in the air flow occurs, as shown in Figs.2 and 3. This suggesta that the surface-renewal motion in the water flow is induced in the front of the wave crest by the strong shear due to the organized motion in the air flow (see Figs.4 and 5). This surface-renewal motion controls the CO_2 transfer across the wavy sheared air-water interface.

4.Conclusions

Turbulence structure and CO_2 transfer mechanism across a wavy sheared air-water interface were numerically investigated in relation to the organized motions in the interface region. The results from this study show that the organized motion in the air flow intermittently appears on the front side of the wave crest and there it induces the surface-renewal motion in the water flow through high shear stress on the interface. The surface-renewal motion controls mass transfer across a wavy sheared air-water interface.

Acknowledgements

The computation was carried out by the super computer SX-3 of the Central for Grobal Environmental Research, National Institute for Environmental Studies.

References

1) S.Komori et al., *J. Fluid Mech.* **249**, 161(1993).
2) S.Komori et al., *J. Fluid Mech.* **203**, 103(1989).
3) S.Komori et al., *AIChE J.* **36**, 957(1990).
4) S.Komori et al., *App. Sci. Res.* **51**, 423(1993).
5) S.Komori et al., *Phys. Fluis A* **5**, 115(1993).

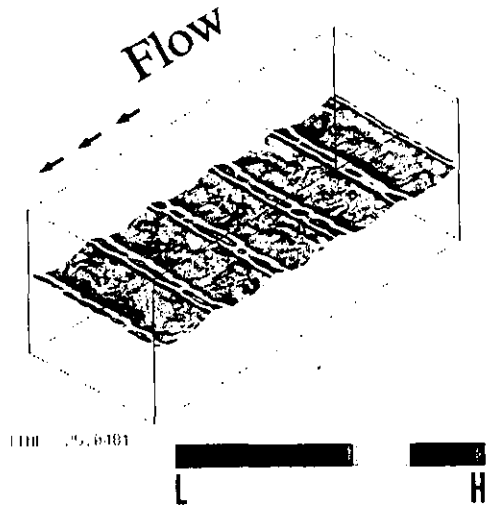

Figure 4: Instantaneous shear stress distribution on the wavy sheared air-water interface.

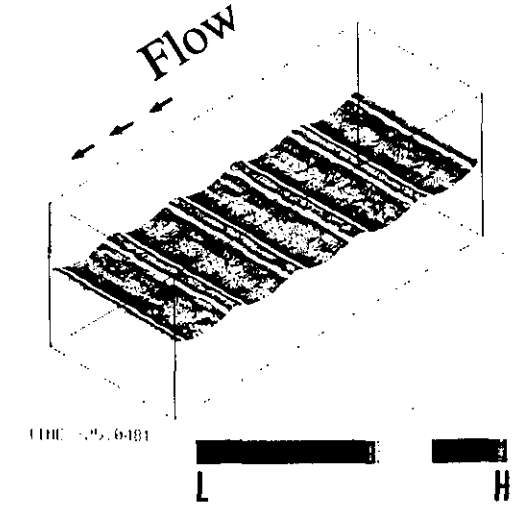

Figure 5: Instantaneous pressure distribution on the wavy sheared air-water interface.